Mitacs Globalink Research Internship Report

Juan Pablo Ortiz Gil

Reaction–diffusion systems with anomalous diffusion
Dr. Yana Nec

Department of Mathematics
Thompson Rivers University
Canada

Chapter 1

Gierer-Meinhardt model

The activator-inhibitor reaction-diffusion system featuring Gierer-Meinhardt kinetics is widely recognized for generating spike-like solutions. In the work presented by [1] a deviation from the conventional formulation of this model is studied, where an integration of sub-diffusion effects is explored. This modified system is examined within the context of a one-dimensional interval, subject to Neumann boundary conditions, and is expressed in the following manner:

$$\begin{aligned} \partial_t^\gamma a &= \epsilon^{2\gamma} a_{xx} - a + \frac{a^p}{h^q}, \qquad -1 < x < 1, \qquad t > 0, \\ \tau \partial_t^\gamma h &= D h_{xx} - h + \epsilon^{-\gamma} \frac{a^m}{h^s}, \qquad -1 < x < 1, \qquad t > 0; \\ a_x(\pm 1, t) &= h_x(\pm 1, t) = 0, \qquad a(x,0) = a_0(x), \qquad h(x,0) = h_0(x). \end{aligned} \tag{1}$$

In this system, the variables $a(x,t)$ and $h(x,t)$ correspond to the concentrations of the activator and inhibitor, respectively. The parameters $\epsilon^{2\gamma}$ and D represent constant diffusivities. The reaction time constant is denoted as $\tau > 0$. The anomaly exponent γ takes values within the range of $0 < \gamma < 1$. The exponents (p, q, m, s) are subject to the relationships

$$p > 1, \quad q > 0, \quad m > 0, \quad s \geq 0, \quad \frac{p-1}{q} < \frac{m}{s+1}.$$

In the limit as ϵ approaches zero, a solution to equation (1) is formulated, characterized by the concentration of the activator at a finite collection of positions x_i with $i = 1, \ldots, n$. This high concentration thereof is referred to as a spike, where each x_i corresponds to the center of the i-th spike. The underlying solution for the activator equation in (1), situated between each spike, adopts the trivial state $a(x,t) \equiv 0$. Within the vicinity of each x_i, an inner coordinate y_i is introduced, defined as

$$y_i(t) = \epsilon^{-\gamma}\big(x - x_i(\sigma)\big),$$

where $\sigma = \epsilon^\alpha t$, with $\alpha = \gamma + 1$. In §2, an asymptotic quasi-equilibrium solution within each inner region for equation (1) is provided as $\epsilon \to 0$.

Chapter 2

Reduced System

2.1 Differential-algebraic (DAE) system

In [1] a mathematical framework is developed to describe the dynamics of a system undergoing sub-diffusion, where an n-spike quasi-equilibrium pattern is observed. This framework involves a set of differential algebraic equations (DAEs) that capture the spike dynamics. The temporal evolution of the i-th spike's center and height, denoted as $x_i(\sigma)$ and $\bar{H}_i(\sigma)$, is determined by the differential-algebraic (DAE) system

$$\bar{H}_i(\sigma) = b_m \sum_{j=1}^{n} \bar{H}_j^{\beta m - s} G(x_i; x_j), \quad b_m = \int_{-\infty}^{\infty} u^m \mathrm{d}y, \tag{2a}$$

$$\operatorname{sgn}\left(\frac{\mathrm{d}x_i}{d\sigma}\right) \left|\frac{\mathrm{d}x_i}{\mathrm{d}\sigma}\right|^{\gamma} = -\frac{q b_m}{(p+1)\bar{H}_i} \left\{ \bar{H}_i^{\beta m - s} \langle G_x \rangle_i + \sum_{\substack{j=1 \\ j \neq i}}^{n} \bar{H}_j^{\beta m - s} G_x(x_i; x_j) \right\} f(p;\gamma). \tag{2b}$$

In this context, u is the homoclinic function defined as the unique solution of the boundary value problem

$$\begin{gathered} u'' - u + u^p = 0, \quad -\infty < y < \infty, \quad u'(0) = 0, \quad u(0) > 0, \quad \lim_{|y| \to \infty} u = 0; \\ u(y) = \left[\left(\frac{p+1}{2} \right) \operatorname{sech}^2 \left(\frac{(p-1)}{2} y \right) \right]^{\frac{1}{p-1}}. \end{gathered} \tag{3}$$

In equation (2b), the parameter β is a combination of the kinetic exponents, $\beta = q/(p-1)$. Additionally, the symbol $\langle G_x \rangle_i$ can be expressed as $\frac{1}{2}\big(G_x(x_i^-; x_i) + G_x(x_i^+; x_i)\big)$. In this context, $G(x; x_i)$ is the Green's function satisfying

$$DG_{xx} - G = -\delta(x - x_i), \quad -1 < x < 1; \qquad G_x(\pm 1; x_i) = 0. \tag{4}$$

Furthermore, the anomaly dependent factor $f(p;\gamma)$ is defined by

$$f(p;\gamma) = \left(\int_{-\infty}^{\infty} u^{p+1} \mathrm{d}y \right) \Big/ \left(\int_{-\infty}^{\infty} u'(y) \mathfrak{D}_y^{\gamma} u \mathrm{d}y \right). \tag{5}$$

The operator $\mathfrak{D}_y^\gamma u$ can be regarded as a propagating fractional derivative and is defined as in Lemma 2.1 of [1]. For the numerical computation, this definition is truncated at y_∞ and regularised using integration by parts to get

$$\begin{aligned}\mathfrak{D}_y^\gamma u(y) =& \frac{y_\infty^{-\gamma}}{\Gamma(1-\gamma)}\mathrm{sgn}x_i'\big(u(y)-u(y+y_\infty\mathrm{sgn}x_i')\big)+\frac{y_\infty^{1-\gamma}}{\Gamma(2-\gamma)}u'(y+y_\infty\mathrm{sgn}x_i')\\ &-\frac{1}{\Gamma(2-\gamma)}\int_y^{y+y_\infty\mathrm{sgn}x_i'}\left(u(\xi)-u^p(\xi)\right)\left((\xi-y)\mathrm{sgn}x_i'\right)^{1-\gamma}\mathrm{d}\xi.\end{aligned}$$

The methodology employed to compute this term is studied in [2].

2.2 Green's function

To solve equation (4), we can separate the space into two sub-intervals, where the following differential equations are valid:

$$\begin{aligned} &DG_{xx}^- - G^- = 0, \quad -1 < x < x_i; \quad G_x^-(-1;x_i) = 0,\\ &DG_{xx}^+ - G^+ = 0, \qquad x_i < x < 1; \quad G_x^+(1;x_i) = 0,\end{aligned} \tag{6}$$

with G^- and G^+ representing the solutions for Green's function in the sub-intervals $(-1, x_i)$ and $(x_i, 1)$ respectively. The solution for (6), introducing the definition $\alpha = D^{-1/2}$, is clearly of the form

$$\begin{aligned} G^- &= C_1^- \sinh(\alpha x) + C_2^- \cosh(\alpha x),\\ G^+ &= C_1^+ \sinh(\alpha x) + C_2^+ \cosh(\alpha x).\end{aligned}$$

To obtain an exact value for the unknowns one must apply boundary and continuity conditions.

2.2.1 Boundary conditions

Let us start with the condition $G_x^-(-1;x_i) = 0$. Substituting this in the proposed solution we can see that

$$G_x^-(-1;x_i) = C_1^-\alpha\cosh(-\alpha) + C_2^-\alpha\sinh(-\alpha) = 0,$$

leading to the condition $C_1^- = C_2^-\tanh(\alpha)$. Therefore

$$\begin{aligned} G^- &= C_2^-\tanh(\alpha)\sinh(\alpha x) + C_2^-\cosh(\alpha x) = C_2^-\,\mathrm{sech}(\alpha)\cosh(\alpha x+\alpha),\\ G^- &= C^-\cosh(\alpha x+\alpha).\end{aligned}$$

Analogously for $G_x^+(1;x_i) = 0$, we obtain the condition $C_1^+ = -C_2^+\tanh(\alpha)$, and therefore

$$\begin{aligned} G^+ &= -C_2^+\tanh(\alpha)\sinh(\alpha x) + C_2^+\cosh(\alpha x) = C_2^+\,\mathrm{sech}(\alpha)\cosh(\alpha x-\alpha),\\ G^+ &= C^+\cosh(\alpha x-\alpha).\end{aligned}$$

2.2.2 Continuity conditions

The solution must satisfy $G^-(x_i;x_i) = G^+(x_i;x_i) \longleftrightarrow \boxed{C^- \cosh(\alpha x_i + \alpha) = C^+ \cosh(\alpha x_i - \alpha)}$. The last condition is derived from the integration of equation (4) around the discontinuity point:

$$\lim_{\epsilon\to 0}\int_{x_i-\epsilon}^{x_i+\epsilon} DG_{xx}\mathrm{d}x - \lim_{\epsilon\to 0}\int_{x_i-\epsilon}^{x_i+\epsilon} G\mathrm{d}x = -\lim_{\epsilon\to 0}\int_{x_i-\epsilon}^{x_i+\epsilon}\delta(x-x_i)\mathrm{d}x,$$

$$\lim_{\epsilon\to 0} DG_x\Big|_{x_i-\epsilon}^{x_i+\epsilon} = -1 \quad \longleftrightarrow \quad G_x^+ - G_x^- = -\frac{1}{D},$$

leading to the condition $\boxed{C^+ \sinh(\alpha x_i - \alpha) - C^- \sinh(\alpha x_i + \alpha) = -\alpha}$. This way we have obtained a set of 2 equations for 2 unknowns that can be solved by direct calculation. From the first boxed condition it is clear that

$$C^- = C^+ \frac{\cosh(\alpha x_i - \alpha)}{\cosh(\alpha x_i + \alpha)}.$$

Then, substituting this result in the integral continuity equation, it follows that

$$C^+ = \frac{\alpha \cosh(\alpha x_i + \alpha)}{\sinh(2\alpha)},$$

and finally we take this to the definition of C^- in terms of C^+, obtaining that

$$C^- = \frac{\alpha \cosh(\alpha x_i + \alpha)}{\sinh(2\alpha)} \frac{\cosh(\alpha x_i - \alpha)}{\cosh(\alpha x_i + \alpha)} = \frac{\alpha \cosh(\alpha x_i - \alpha)}{\sinh(2\alpha)}.$$

Therefore, the Green function is

$$G(x;x_i) = \begin{cases} \dfrac{\alpha \cosh(\alpha x_i - \alpha)}{\sinh(2\alpha)} \cosh(\alpha x + \alpha), & -1 < x < x_i; \\ \dfrac{\alpha \cosh(\alpha x_i + \alpha)}{\sinh(2\alpha)} \cosh(\alpha x - \alpha), & x_i < x < 1; \end{cases} \tag{7}$$

with $\alpha = D^{-1/2}$.

2.3 Integrals

2.3.1 Weight factor b_m

An analytical expression for b_m in equation (2a) is obtained by substituting u^m as defined in equation (3):

$$b_m = \int_{-\infty}^{\infty} u^m \mathrm{d}y = \frac{4}{p-1}\left(\frac{p+1}{2}\right)^{\frac{m}{p-1}} \int_0^{\infty} \cosh^{-\frac{2m}{p-1}}(v)\mathrm{d}v.$$

The exact solution for the integral is obtained in Appendix B of [3]. Incorporating that solution into our expression, we obtain that

$$b_m = \frac{2}{p-1}\left(\frac{p+1}{2}\right)^{\frac{m}{p-1}} B\left(\frac{1}{2}, \frac{m}{p-1}\right), \tag{8}$$

where $B(\mu, \nu)$ is the beta function, computed via definition **8.384** of [4]:

$$B(\mu, \nu) = \frac{\Gamma(\mu)\Gamma(\nu)}{\Gamma(\mu+\nu)}.$$

With these relations, the value of b_m can be explicitly computed in C.

2.3.2 Anomaly dependent factor

The calculation of the numerator of the component $f(p;\gamma)$ follows a similar approach as for b_m, particularly when setting m equal to $p+1$. This section focuses on the computation of the denominator in equation (5), which requires truncation at y_∞:

$$\int_{-\infty}^{\infty} u'(y)\mathfrak{D}_y^\gamma u dy = \int_{-\infty}^{y_\infty} u'(y)\mathfrak{D}_y^\gamma u dy + \int_{-y_\infty}^{y_\infty} u'(y)\mathfrak{D}_y^\gamma u dy + \int_{-y_\infty}^{\infty} u'(y)\mathfrak{D}_y^\gamma u dy.$$

In [1] it is demonstrated that $\mathfrak{D}_y^\gamma u$ tends to zero as y tends to $\pm y_\infty$. This result allows us to disregard the influence of the tails in the complete calculation, leading to the trucated expression

$$\int_{-\infty}^{\infty} u'(y)\mathfrak{D}_y^\gamma u dy \approx \int_{-y_\infty}^{y_\infty} u'(y)\mathfrak{D}_y^\gamma u dy.$$

The computation process for various values of p and γ is implemented in the programming language C. Specifically, p ranges from 1.5 to 4.5 with intervals of 0.5, and γ ranges from 0.1 to 0.9 with intervals of 0.1. These values were chosen to be consistent with reasonable chemical systems and in compatibility with [2].

```c
/* algorithm employed for memory allocation */
void f2allocate(long int n,double* *A)
{ /* allocate and initialise a double one-dimensional array */
 if((*A=(double*)calloc(n,sizeof(double)))==NULL){
   printf("Out of memory.\n");
   exit(-1);
 }
}

void memory(long int n, double* *det)
{
 f2allocate(n,det);
}
```

For γ values between 0.1 and 0.4, the program employs memory allocation to calculate $\mathfrak{D}_y^\gamma u$ over the range from $-y_\infty$ to y_∞ using Simpson's method. The number of subdivisions for Simpson's method is determined using the results from [2], where the calculation was optimized to mantain a precision of 10^{-10}. Subsequently, the program employs Simpson's method again with 100 subdivisions to calculate the outer integral, retrieving the required values of $\mathfrak{D}_y^\gamma u$ from the allocated array. It then iteratively refines the calculation using an increasing number of subdivisions until the difference converges to an order of 10^{-10}. This way the same precision is mantained throughout the entire simulation.

```
/* number of sub-divisions obtained in [2] */
long int n = 2.0*n_approx_general(5.0,p,g);

/* memory allocation and Du calculation*/
memory(n+1,&det);
double index = 0.0;
double i = -5.0;
double stepSize = (5.0 - (-5.0))/n;

while (i < 5.0){
 index = (5.0 + i) / stepSize;
 det[(int)round(index)] = integrand2(i,p,g);
 i = i + stepSize;
}

/* outer integral calculation */
//Simpson method retrieving Du values from array
anom_in = simpson2(-5.0,5.0,100,p,g,m,det);

for (int j = 100; j<=n/2.0; j*=2){
 anom = simpson2(-5.0,5.0,2*j,p,g,m,det);
 if (fabs(anom-anom_in) < pow(10,-9)){
  break;
 }
 anom_in = anom;
}

free(det);
```

For γ values in the range of 0.5 to 0.9, the program follows a similar approach, but in this case, it calculates specific values of $\mathfrak{D}_y^\gamma u$ on spot as needed, without utilizing memory allocation. This decision arises from the observation that the number of subdivisions calculated in [2] for these specific γ values tends to be too large. Through testing, it was discovered that for higher γ values, the outer integral's subdivision count didn't need to be as extensive. Consequently, this modification substantially reduces the computation time while maintaining accurate results.

```
/* outer integral calculation */
//Simpson method calculating Du on-the-fly
anom_in = simpson2_big(-5.0,5.0,100,p,g,m,integrand2);

```

```
for (int k = 100; k<=n; k*=2){
 anom = simpson2_big(-5.0,5.0,2*k,p,g,m,integrand2);
 if (fabs(anom-anom_in) < pow(10,-9)){
  break;
 }
 anom_in = anom;
}
```

By employing the results obtained from these computational procedures, the anomaly dependent factor is calculated for every combination of p and γ. The resulting outcome showcases a reduction in data points while achieving enhanced precision relative to the portrayal in Figure 2 of [1].

2.4 Numerical scheme

To approximate the solution of the initial-value problem, we need to transform equation (2b) into the form

$$x_i' = g(\sigma, x_i), \qquad \sigma_0 \leq \sigma \leq \sigma_n, \qquad x_i(\sigma_0) = \eta,$$

and then apply the fourth-order Runge-Kutta method. For this purpose, the following variables are defined:

$$\begin{aligned}
w_j &= x_i(\sigma_j), \\
k_1 &= hg\big(\sigma_j, x_i(\sigma_j)\big), \\
k_2 &= hg\left(\sigma_j + \frac{h}{2}, x_i(\sigma_j) + \frac{1}{2}k_1\right), \\
k_3 &= hg\left(\sigma_j + \frac{h}{2}, x_i(\sigma_j) + \frac{1}{2}k_2\right), \\
k_4 &= hg\big(\sigma_{j+1}, x_i(\sigma_j) + k_3\big).
\end{aligned}$$

Here, $w_0 = \eta = x_1(\sigma_0)$ serves as the initial condition, and $h = (\sigma_n - \sigma_0) = \epsilon^\alpha(t_n - t_0)$. With these definitions, the algorithm to use for obtaining the values of $x_i(\sigma)$ over time becomes:

$$w_{j+1} = w_j + \frac{1}{6}\left(k_1 + 2k_2 + 2k_3 + k_4\right).$$

2.5 One-spike pattern

2.5.1 Problem formulation

For a quasi-equilibrum pattern of a single spike centered at x_1, the DAE system (2a, 2b) can be simplified to

$$\bar{H}_1(\sigma) = b_m \bar{H}_1^{\beta m - s} G(x_1; x_1), \tag{9a}$$

$$\operatorname{sgn}\left(\frac{\mathrm{d}x_1}{\mathrm{d}\sigma}\right)\left|\frac{\mathrm{d}x_1}{\mathrm{d}\sigma}\right|^{\gamma} = -\frac{q b_m}{(p+1)\bar{H}_1}\left[\bar{H}_1^{\beta m - s}\langle G_x\rangle_1\right] f(p;\gamma). \tag{9b}$$

Let's analyze the right-hand side of the differential equation (9b). The values q, p, β, m, b_m, $f(p;\gamma)$ are constants or constant dependent values, so they are grouped together. Additionaly, from the algebraic equation in (9a), we have that

$$\bar{H}_1^{\beta m - s - 1} = \frac{1}{b_m G(x_1; x_1)},$$

and since Green's function is as defined in equation (7):

$$\frac{\langle G_x\rangle_1}{G(x_1; x_1)} = \frac{\alpha \sinh(2\alpha x_1)}{\cosh(2\alpha x_1) + \cosh(2\alpha)}.$$

Upon substitution, equation (9b) takes the form:

$$\operatorname{sgn}\left(\frac{\mathrm{d}x_1}{\mathrm{d}\sigma}\right)\left|\frac{\mathrm{d}x_1}{\mathrm{d}\sigma}\right|^{\gamma} = -\frac{q f(p;\gamma)\alpha}{(p+1)}\left[\frac{\sinh(2\alpha x_1)}{\cosh(2\alpha x_1) + \cosh(2\alpha)}\right],$$

which is equivalent to

$$\frac{\mathrm{d}x_1}{\mathrm{d}\sigma} = \operatorname{sgn}\left(\frac{\mathrm{d}x_1}{\mathrm{d}\sigma}\right)\left[-\operatorname{sgn}\left(\frac{\mathrm{d}x_1}{\mathrm{d}\sigma}\right)\frac{q f(p;\gamma)\alpha}{(p+1)}\frac{\sinh(2\alpha x_1)}{\cosh(2\alpha x_1) + \cosh(2\alpha)}\right]^{1/\gamma}. \tag{10}$$

We must ensure that the expression under the root is positive, so we separate equation (10) in two parts. First, we impose the condition $\frac{\mathrm{d}x_1}{\mathrm{d}\sigma} < 0$. This way, the start point is at the right side of the equilibrium point, resulting in the equation:

$$\frac{\mathrm{d}x_1}{\mathrm{d}\sigma} = -\left[\frac{q f(p;\gamma)\alpha}{(p+1)}\frac{\sinh(2\alpha x_1)}{\cosh(2\alpha x_1) + \cosh(2\alpha)}\right]^{1/\gamma}.$$

Now, by imposing the condition $\frac{\mathrm{d}x_1}{\mathrm{d}\sigma} > 0$, with the start point at the left side of the equilibrium point, we obtain

$$\frac{\mathrm{d}x_1}{\mathrm{d}\sigma} = \left[-\frac{q f(p;\gamma)\alpha}{(p+1)}\frac{\sinh(2\alpha x_1)}{\cosh(2\alpha x_1) + \cosh(2\alpha)}\right]^{1/\gamma}.$$

In both cases, equation (10) satisfies the form $x_1' = g(\sigma, x_1)$, incorporating non-linear terms. Finally, to complete the solution of the DAE system (9a, 9b)

$$\bar{H}_1(\sigma) = \left[\frac{b_m \alpha}{2}\frac{\cosh(2\alpha x_1) + \cosh(2\alpha)}{\sinh(2\alpha)}\right]^{1/1+s-\beta m}.$$

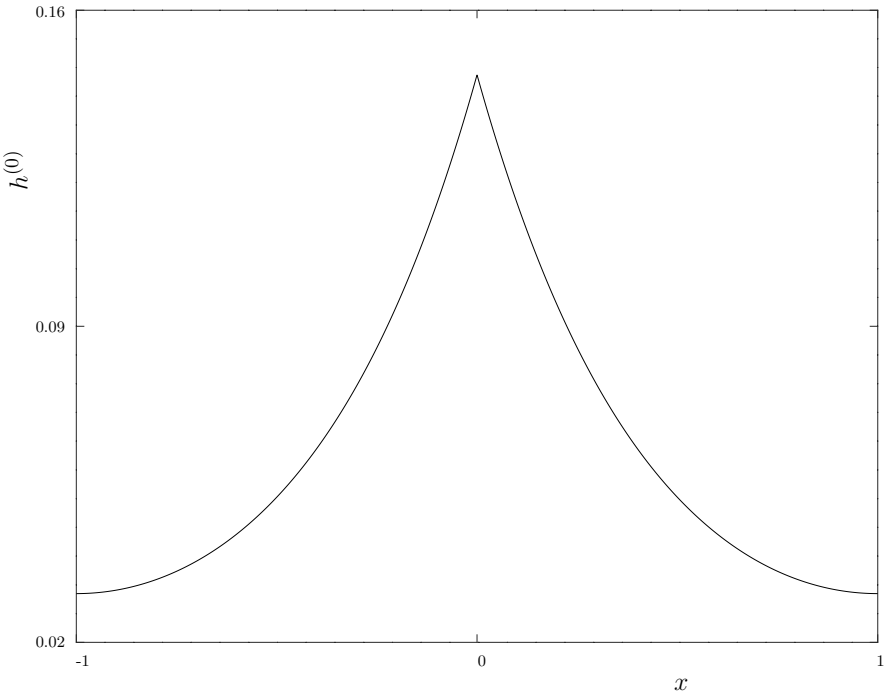

Figure 2.1: Inhibitor concentration in space $\big($see equation (11)$\big)$ for one spike pattern. The system parameters used are $p = 2$, $\gamma = 0.9$ and $D = 0.2$.

2.5.2 Solution

To solve the system, the algorithm described in Section 2.4 was employed. A typical case results are shown in Figure 2.1 and Figure 2.2, depicting the inhibitor concentration in space and the drifting behavior of the center of the spike over time, respectively. The inhibitor concentration in space was determined using the equation:

$$h^{(0)}(x,t) = b_m \sum_{i=i}^{n} \bar{H}_i^{\beta m - s} G(x; x_i), \tag{11}$$

which is a result taken from [1]. In particular, concerning the drifting behavior, curves were generated for $\epsilon = 0.5$, 0.25, and 0.1, and these were compared against the linearized solution $\big($where equation (10) was linearized around the equilibrium point, $x_1 = 0$, for this purpose$\big)$. It becomes evident from the comparison that as ϵ decreases, the solution approximates the linearized result more accurately. This observation highlights that smaller ϵ values yield superior solutions, as expected for an asymptotic solution.

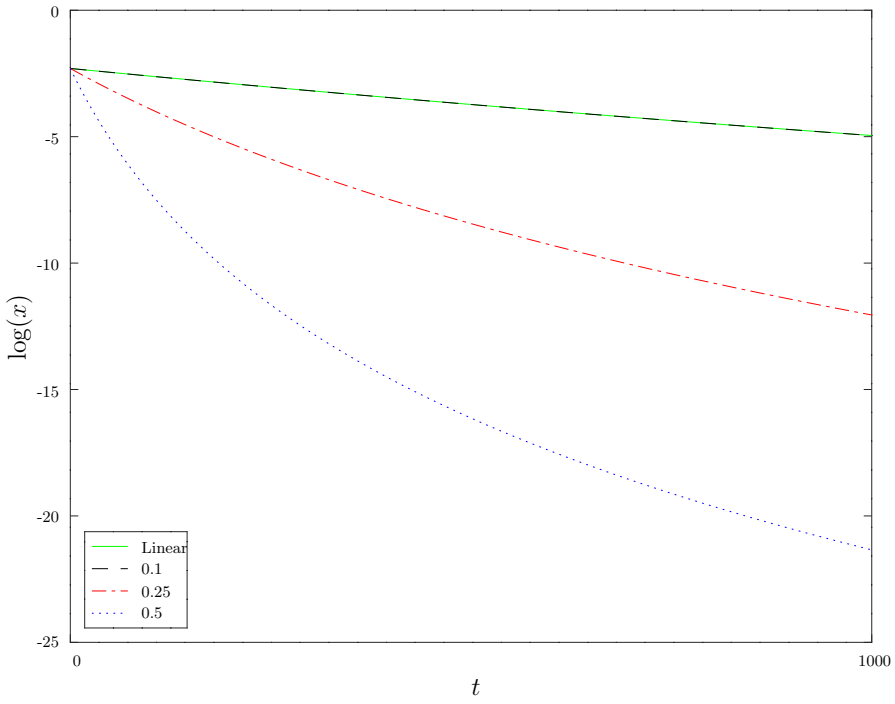

Figure 2.2: Drifting of one spike for several values of ϵ (see legend). The system parameters are as in Figure 2.1, with $D = 1$.

2.6 Two-spike pattern

2.6.1 Problem formulation

In the case of a quasi-equilibrium pattern featuring two spikes centered at x_1 and x_2, with the condition that $-1 < x_2(\sigma) < x_1(\sigma) < 1$, the DAE system (2a, 2b) can be simplified to:

$$\begin{aligned}
\operatorname{sgn}\left(\frac{\mathrm{d}x_1}{\mathrm{d}\sigma}\right)\left|\frac{\mathrm{d}x_1}{\mathrm{d}\sigma}\right|^{\gamma} &= -\frac{qb_m}{(p+1)\bar{H}_1}\left\{\bar{H}_1^{\beta m-s}\langle G_x\rangle_1 + \bar{H}_2^{\beta m-s}G_x(x_1;x_2)\right\} f(p;\gamma), \\
\operatorname{sgn}\left(\frac{\mathrm{d}x_2}{\mathrm{d}\sigma}\right)\left|\frac{\mathrm{d}x_2}{\mathrm{d}\sigma}\right|^{\gamma} &= -\frac{qb_m}{(p+1)\bar{H}_2}\left\{\bar{H}_2^{\beta m-s}\langle G_x\rangle_2 + \bar{H}_1^{\beta m-s}G_x(x_2;x_1)\right\} f(p;\gamma),
\end{aligned} \tag{12}$$

where these equations describe the temporal evolution of the centers of the spikes. Similarly, for the spike's heights we have that

$$\begin{aligned}
\bar{H}_1(\sigma) &= b_m\left\{\bar{H}_1^{\beta m-s}G(x_1;x_1) + \bar{H}_2^{\beta m-s}G(x_1;x_2)\right\}, \\
\bar{H}_2(\sigma) &= b_m\left\{\bar{H}_1^{\beta m-s}G(x_2;x_1) + \bar{H}_2^{\beta m-s}G(x_2;x_2)\right\}.
\end{aligned} \tag{13}$$

For the specific scenario of a symmetric two-spike quasi-equilibrium solution where $x_2 = -x_1$ holds at all times, our attention can be directed to just one of the spikes. This allows us to simplify the ordinary differential equations (ODEs) in equation (12) to:

$$\operatorname{sgn}\left(\frac{\mathrm{d}x_1}{\mathrm{d}\sigma}\right)\left|\frac{\mathrm{d}x_1}{\mathrm{d}\sigma}\right|^{\gamma} = -\frac{qb_m}{(p+1)\bar{H}_1}\left\{\bar{H}_1^{\beta m-s}\langle G_x\rangle_1 + \bar{H}_2^{\beta m-s}G_x(x_1;-x_1)\right\} f(p;\gamma).$$

Another result of major importance in order to find a solution to the system is the relation between the spike's heights. By subtracting the equations in (13), we arrive at the expression

$$\bar{H}_1 - \bar{H}_2 = b_m\left[G(x_1;x_1) - G(-x_1;x_1)\right]\left(\bar{H}_1^{\beta m-s} - \bar{H}_2^{\beta m-s}\right).$$

Both sides are related by a positive constant, therefore upon a proper scaling we can absorb it into H_i and look at just:

$$\bar{H}_1 - \bar{H}_2 = \bar{H}_1^{\alpha} - \bar{H}_2^{\alpha}.$$

We designate one solution as $\bar{H}_1 = \bar{H}_2$ and the other as the unique solution of

$$\bar{H}_1 - \bar{H}_2 - \bar{H}_1^{\alpha} + \bar{H}_2^{\alpha} = 0; \qquad \bar{H}_1 \neq \bar{H}_2.$$

This is studied by plotting the surface $f\left(\bar{H}_1, \bar{H}_2\right) = \bar{H}_1 - \bar{H}_2 - \bar{H}_1^{\alpha} + \bar{H}_2^{\alpha}$ and its intersection with the plane $f\left(\bar{H}_1, \bar{H}_2\right) = 0$, as depicted in Figure 2.3.

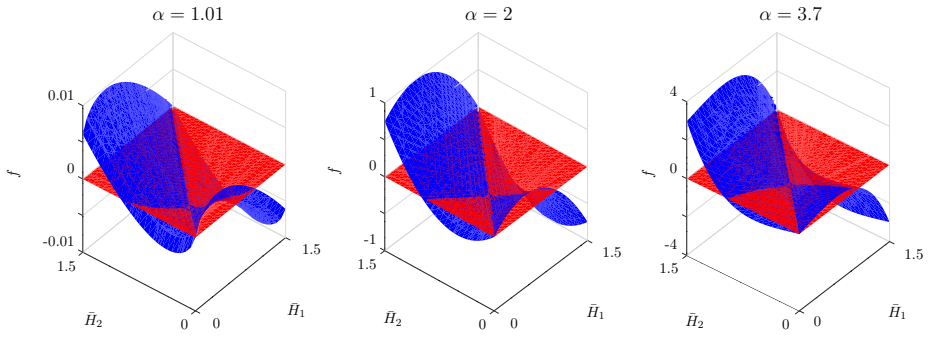

Figure 2.3: Surface $f\left(\bar{H}_1, \bar{H}_2\right)$ for several values of α. The solutions mentioned are evident as the intersection curves between the red and blue surfaces. Note that as $\bar{H}_1$ increases, the surface approaches $-\infty$, while as $\bar{H}_2$ increases, the surface tends towards ∞ for all considered cases.

Here, we will concentrate on the solution $\bar{H}_1 = \bar{H}_2$. With this in mind, let's analyze the right-hand side of equation (12). From equation (13) we deduce that

$$\bar{H}_1^{\beta m-s-1} = \frac{1}{b_m\left\{G(x_1;x_1) + G(-x_1;x_1)\right\}},$$

and since Green's function is as defined in equation (7), it follows that

$$\frac{\langle G_x\rangle_1}{G(x_1;x_1)+G(-x_1;x_1)} = \frac{\alpha\sinh(2\alpha x_1)}{4\cosh(\alpha x_1-\alpha)\cosh(\alpha)\cosh(\alpha x_1)},$$
$$\frac{G_x(x_1;-x_1)}{G(x_1;x_1)+G(-x_1;x_1)} = \frac{\alpha\sinh(\alpha x_1-\alpha)}{2\cosh(\alpha)\cosh(\alpha x_1)}.$$

Simplifying further, we obtain:

$$\frac{\sinh(2\alpha x_1)}{4\cosh(\alpha x_1-\alpha)\cosh(\alpha)\cosh(\alpha x_1)}+\frac{\sinh(\alpha x_1-\alpha)}{2\cosh(\alpha)\cosh(\alpha x_1)} = -\frac{1}{2}\big[\tanh(\alpha-\alpha x_1)-\tanh(\alpha x_1)\big].$$

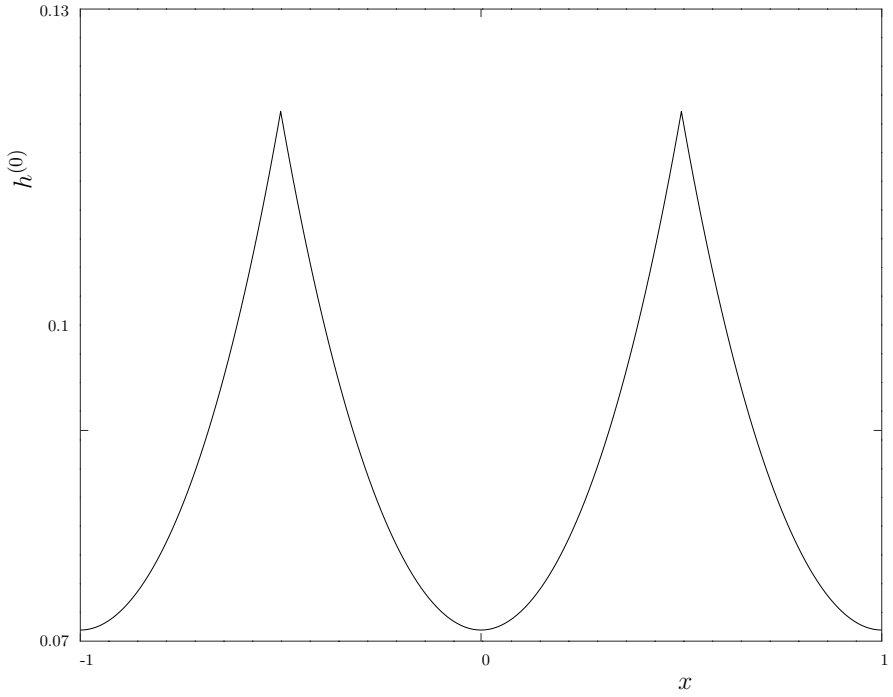

Figure 2.4: Inhibitor concentration in space $\big($see equation (11)$\big)$ for a two spike pattern. The system parameters used are $p = 2$, $\gamma = 0.9$ and $D = 0.2$.

Then, these results are substituted into the differential equation, obtaining that

$$\operatorname{sgn}\left(\frac{\mathrm{d}x_1}{\mathrm{d}\sigma}\right)\left|\frac{\mathrm{d}x_1}{\mathrm{d}\sigma}\right|^{\gamma} = \frac{qf(p;\gamma)\alpha}{2(p+1)}\big[\tanh(\alpha-\alpha x_1)-\tanh(\alpha x_1)\big],$$

which is equivalent to

$$\frac{\mathrm{d}x_1}{\mathrm{d}\sigma} = \operatorname{sgn}\left(\frac{\mathrm{d}x_1}{\mathrm{d}\sigma}\right)\left[\operatorname{sgn}\left(\frac{\mathrm{d}x_1}{\mathrm{d}\sigma}\right)\frac{qf(p;\gamma)\alpha}{2(p+1)}\big(\tanh(\alpha-\alpha x_1)-\tanh(\alpha x_1)\big)\right]^{1/\gamma}. \qquad (14)$$

We must ensure that the expression under the root is positive, so we separate equation (14) in two parts. First, we impose the condition $\frac{dx_1}{d\sigma} < 0$. This way, the start point is at the right side of the equilibrium point, resulting in the equation:

$$\frac{\mathrm{d}x_1}{\mathrm{d}\sigma} = -\left[\frac{qf(p;\gamma)\alpha}{2(p+1)}\big(\tanh(\alpha x_1) - \tanh(\alpha - \alpha x_1)\big)\right]^{1/\gamma}.$$

Now, by imposing the condition $\frac{\mathrm{d}x_1}{\mathrm{d}\sigma} > 0$, with the start point at the left side of the equilibrium point, we obtain

$$\frac{\mathrm{d}x_1}{\mathrm{d}\sigma} = \left[-\frac{qf(p;\gamma)\alpha}{2(p+1)}\big(\tanh(\alpha x_1) - \tanh(\alpha - \alpha x_1)\big)\right]^{1/\gamma}.$$

In both cases, equation (14) satisfies the form $x_1' = g(\sigma, x_1)$, incorporating non-linear terms. Finally, to complete the solution of the DAE system of equations (12) and (13)

$$\bar{H}_1(\sigma) = \left[\frac{b_m\alpha}{\tanh(\alpha x_1) + \tanh(\alpha - \alpha x_1)}\right]^{1/1+s-\beta m}.$$

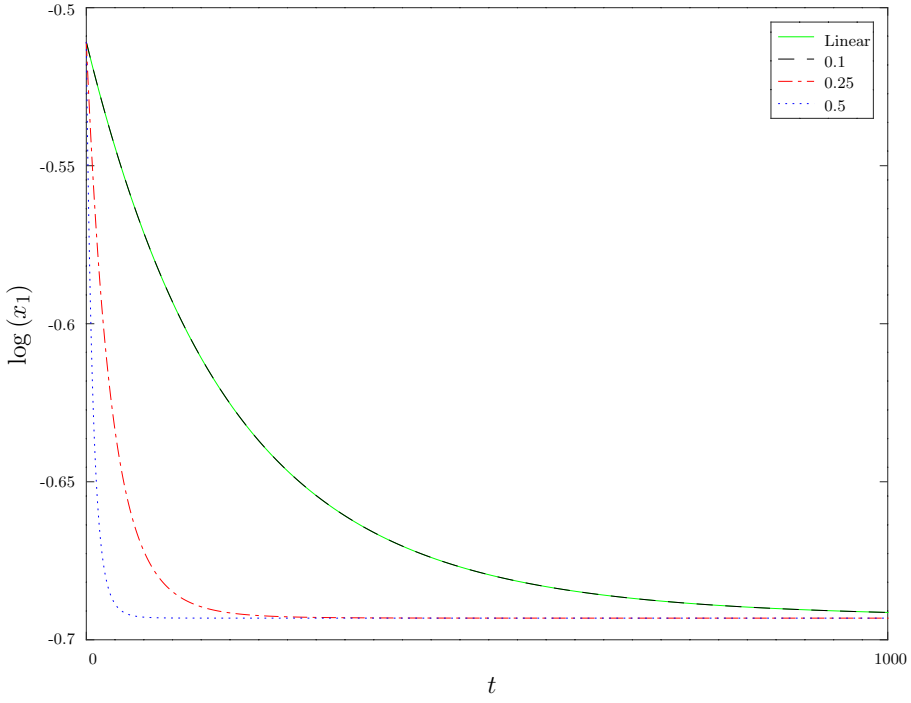

Figure 2.5: Drifting of one of the symmetric spikes (denoted as x_1) for several values of ϵ (see legend). The system parameters are as in Figure 2.4, with $D = 1$.

2.6.2 Solution

To solve the system, the algorithm described in Section 2.4 was employed. A typical case results are shown in Figure 2.4 and Figure 2.5, depicting the inhibitor concentration in space and the drifting behavior of the center of the one of the spikes over time, respectively. The inhibitor concentration in space was determined using equation (11).

In particular, concerning the drifting behavior, curves were generated for $\epsilon = 0.5$, 0.25, and 0.1, and these were compared against the linearized solution $\big($where equation (14) was linearized around the equilibrium point, $x_1 = 0.5$, for this purpose$\big)$. As for one spike, it becomes evident that as ϵ decreases, the solution approximates the linearized result more accurately.

Bibliography

[1] Nec, Yana and Ward, Michael J. "Dynamics and stability of spike-type solutions to a one dimensional Gierer–Meinhardt model with sub-diffusion". In: *Physica D: Nonlinear Phenomena* 241.10 (2012).

[2] Nehemie Nguimbous. *Numerical approximation of $\mathfrak{D}_y^\gamma u$ with a controlled precision*. Report. Thompson Rivers University, 2023.

[3] Booker, Kyle and Nec, Yana. "On accuracy of numerical solution to boundary value problems on infinite domains with slow decay". In: *Math. Model. Nat. Phenom.* 14.5 (2019).

[4] I.S. Gradshteyn and I.M. Ryzhik. *Table of Integrals, Series, and Products*. Ed. by Alan Jeffrey and Daniel Zwillinger. Seventh Edition. Academic Press, 2007.